A primer for resonant tunnelling

Jérémy Le Deunff, Olivier Brodier, Amaury Mouchet

A primer for resonant tunnelling

Jérémy Le Deunff[2], Olivier Brodier[1] & Amaury Mouchet[1]

[1]Laboratoire de Mathématiques et Physique Théorique,
Université François Rabelais de Tours — CNRS (UMR 6083),
Fédération Denis Poisson,
Parc de Grandmont 37200 Tours, France.
brodier, mouchet @lmpt.univ-tours.fr

[2]Max-Planck-Institut für Physik komplexer Systeme,
Nöthnitzer Straße 38,
01187 Dresden, Germany.
deunff@pks.mpg.de

September 27, 2012

PACS: 05.45.Mt, 03.65.Sq, 03.65.Xp, 05.60.Gg

Abstract

Resonant tunnelling is studied numerically and analytically with the help of a three-well quantum one-dimensional time-independent model. The simplest cases are considered where the three-well potential is polynomial or piecewise constant.

1 Introduction

Even though the expression "tunnel effect" was coined for the first time in 1931 by Schottky in German, ("Wellenmechanische Tunneleffekt", according to Merzbacher, 2002), the importance of the quantum transmission through a potential barrier at an energy below its maximum was acknowledged immediately after quantum mechanics reached its maturity in 1926. Indeed, Hund published the first papers on tunnelling in 1927 where a one-dimensional double-well was introduced to modelise chemical binding (Hund, 1927a) and the deformation potential of a NH_3-like molecule (Hund, 1927b). In the latter article, Hund obtained the crucial point that tunnelling was exponentially sensitive to the characteristic parameters of the barrier. The very same year, tunnelling was first considered in unbounded models by Nordheim (1927) to describe the electronic emission from metals. One year later, Fowler & Nordheim (1928) successfully described how this emission was driven by high electric field and Gamow (1928), Gurney & Condon (1928) showed how tunnelling was involved in the α-decay of some radioactive nuclei; in both cases, the exponential dependence of the decay

rates with energy was explained by tunnelling through a one-dimensional barrier that modelled the mean attractive field created respectively by the metal and the nucleons (and the latters were still unknown in 1928).

Such tunnelling models can be introduced very early in a first course on quantum mechanics. As soon as the stationnary Schrödinger equation is presented together with the constraints imposed on its resolution (normalisation, smoothness of the solutions), tunnelling can be understood as a direct consequence of the wavy nature of quantum particles. For usual textbooks treatments see for instance (Bohm, 1951, § 11.5), (Messiah, 1959, chap. III, § 7), (Merzbacher, 1970, chaps. 5 and 6). Probably more striking for the beginners than the quantization of the energy levels of a bounded system, tunnelling provides a first contact with the strangeness of quantum phenomena, even for those already familiar with evanescent waves in optics.

Tunnelling has nowadays been extended to qualify *any quantum process that is forbidden by real solutions of classical equations*[1]; thus, since a quantum/classical comparison is somehow necessary, it is, by definition, a phenomenon that occurs in the semiclassical limit, where formally $\hbar \to 0$ (physically this corresponds to large classical actions compared to the Planck constant. This limit is not trivial : from the Schrödinger equation we can see that the value $\hbar = 0$ is singular; however, in practice, the semiclassical approximation works quite well even for relatively large value of $\hbar$. The only requirement in our case is that $\hbar$ must remain small enough to get two almost degenerate eigenvalues below the tunnelling barrier.) With the help of approximate methods of resolution of ordinary differential equation that were originally developed by Jeffreys (1925), Kramers (1926), Brillouin (1926), Wentzel (1926)—the so-called JWKB approximation that provide $\hbar$ asymptotic expansions for the quantum quantities (for a rigourous though accessible presentation with more details than the ones usually presented in quantum mechanics textbooks see Bender & Orszag, 1978, chap. 10)—one may also gain some insight of how subtle the transition between the classical and the quantum world occurs. However, from the singular behaviour of the wave functions (in their semiclassical amplitudes near the classical turning points and, in any case, in their phases), it appears immediately that the semiclassical limit $\hbar \to 0$ is not as simple as the other familiar limit $c \to \infty$ that describes the transition towards non-relativistic theories (physically this corresponds to small classical velocities compared to the speed of light c).

Remaining at an introductory level, within JWKB approximation, it is quite simple to justify the exponential form taken by the transmission factor τ (defined to be the square of the ratio between the amplitudes of the outgoing and incoming waves) of one barrier like the one depicted in figure 1a) (Bohm, 1951, § 12.13), (Landau & Lifshitz, 1958, § 50, eq. (50.5)), (Messiah, 1959, chap. VI, § 10 and exercise 5) (Merzbacher, 1970, chap. 7, eq. (7.33))

$$\tau \underset{\hbar \to 0}{\sim} \alpha \, \mathrm{e}^{-2A/\hbar} \, , \tag{1}$$

or the tunnelling beating period $T = \hbar/\Delta E$ in a symmetric double-well like the one given in figure 1b), (Landau & Lifshitz, 1958, § 50, problem 3). In that

[1] For more than one degree of freedom or for time-dependent systems, the interdiction may come from constraints other than the energy conservation. If we look at the dynamics in the phase-space and make the canonical transformation that exchanges position with momenta, it also appears that the reflexion above a barrier can be considered as a tunnelling process.

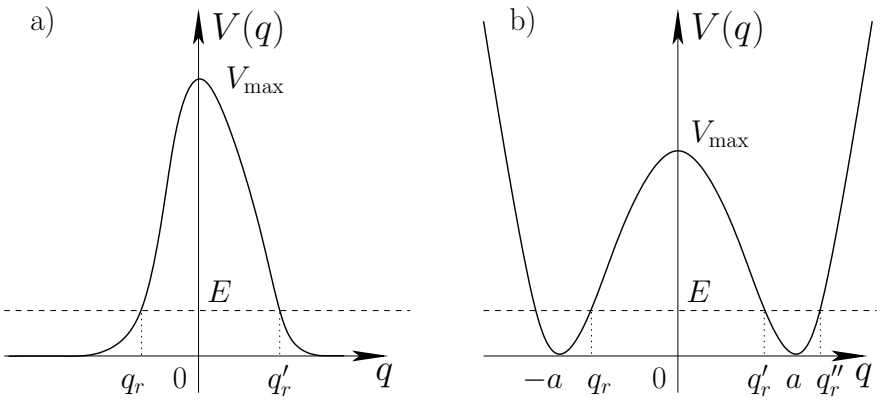

Figure 1: a) One simple potential barrier and b) the double-well potential provide the first illustrations of tunnelling in one dimension.

latter case, tunnelling appears as a coupling between two states localised in the two wells that lifts the degeneracy of their energy. Actually, below the maximum of the barrier $V_{\max}$ the symmetric and antisymmetric exact eigenvalues come by pairs E_n^+ and E_n^- labelled by a finite number of integers $n = 0, 1, ..., N$ and the splitting of the nth doublet is given by

$$\Delta E_n \stackrel{\text{def}}{=} |E_n^+ - E_n^-| \underset{\hbar\to 0}{\sim} \alpha\, \hbar\, \mathrm{e}^{-A/\hbar}\,. \tag{2}$$

It requires some skill to get the correct prefactors α (Garg, 2000) but if we do not bother about them, the above expressions can be straightforwardly obtained. In both cases A is the classical action "under the barrier $V(q)$" of the particle with mass m, more precisely the imaginary part of the action computed with one branch of the imaginary momentum:

$$A(E) \stackrel{\text{def}}{=} \int_{q_r(E)}^{q'_r(E)} \sqrt{2m\big(V(q)-E\big)}\,\mathrm{d}q\,, \tag{3}$$

where q_r and q'_r are the positions of the turning points at the energy E at which the barrier penetration occurs. In the double well case, E is the average energy of the tunnelling doublet $E_n = (E_n^+ + E_n^-)/2$ and may be determined semiclassically within one well by the Einstein-Brillouin-Keller quantization condition (Bohm, 1951, § 11.5), (Landau & Lifshitz, 1958, § 48), (Messiah, 1959, chap. VI,§ 11), (Merzbacher, 1970, chap. 7,§ 3),

$$\oint_{\substack{\text{closed trajectory}\\ \text{at energy } E}} p(q)\,\mathrm{d}q \;=\; 2\pi\hbar\Big(n+\frac{1}{2}\Big) \tag{4}$$

$$\;=\; 2\int_{q'_r(E)}^{q''_r(E)} \sqrt{2m\big(E-V(q)\big)}\,\mathrm{d}q\,, \tag{5}$$

where $q''_r(E)$ stands for the most right turning point at energy E.

Simple exponential laws like (1) or (2), discovered by the pioneers of tunnelling mentioned above, are advantageously used in many applications, most notably the principle of the scanning tunnelling microscope (or rather nanoscope) (Eigler & Schweizer, 1990). However, when the potential has a richer structure than just one bump, even when staying in one dimension, strong deviations by several order of magnitude on the transmission or on the splitting are to be expected. For instance, even if the transmission of one barrier can be made arbitrarily small because of (1), the total transmission factor of two such successive bumps may be enhanced up to its maximum value 1. This resonance tunnelling has fundamentally the same roots than the resonance scattering by one well (Bohm, 1951, chap. 11,§ 7), (Messiah, 1959, chap. III, § 6) (Merzbacher, 1970, chap. VI, § 8): an enhancement is produced by the constructive interference of waves reflected back and forth in between the two bumps. In optics such a coherent superposition of "trapped" electromagnetic waves is the principle of the Fabry-Pérot interferometer (Born & Wolf, 1980, § 7.6). Though accessible with no more technical nor conceptual tools than the ones involved in the JWKB derivation of (1), (2) and (4), quantum analogous treatment of the Fabry-Pérot effect is scarcely treated in the introductory literature (Bohm, 1951, chap. 12, §§ 14-17), see Granot's (2006) recent publication in this journal. The aim of the present article is to fill a gap and complete the study of resonant tunnelling by considering the spectrum of bounded systems rather than scattering. Multidimensionnal tunnelling (including time-dependent one-dimensional systems) requires theoretical tools far beyond the readership's interest of the present journal and is still the subject of an intense research field. However, recent studies has shown that resonant tunnelling (mainly in bounded systems) paved the road to a better understanding of tunnelling in complex systems (Schlagheck et al, 2011). For instance, the huge fluctuations by several orders of magnitude in some tunnelling doublets are precisely of the same origin than the resonance that will be carefully described in the present article. We will remain with a one-dimensional static potential V and choose two tractable models that involve three wells. First (section 2) we will consider a smooth potential, the simplest one being given by a polynomial of degree 6. One of its advantage is that the spectrum can be numerically computed with very fine precision at low cost. Then (section 3) we will introduce another model where V is a piecewise constant which will allow us to go further in the analytical computations. Comparison between the two will strengthen the interpretation of resonnant tunnelling in terms of avoided degeneracies in the spectrum and will show that the Fabry-Pérot effect provides a correct interpretation. The two models encapsulate the same physics and, indeed, their comparison may help to support this intuition. What seems more interesting for pedagogical sake is to consider the opposite way : starting with the intuition that the two models are physically qualitatively equivalent, the very different methods to study them (numerics, level dynamics, Husimi distribution for the smooth case and analytical computations, semiclassics, transfer matrices for the other one) appear to be complementary and mutually supporting.

All along this paper, we will use mainly physical concepts and mathematical tools that correspond to a undergraduate course on quantum physics. However, the accumulation of different techniques (specially the somehow lengthy computations of section 3.2, a reasonable skill in asymptotic expansions, the numerical implementation and the notion of quasiclassical states) are more accessible once

the very first notions of quantum physics are well-understood or during a special supervised training course.

2 Three-well polynomial potential

2.1 Presentation

The simplest smooth symmetric one-dimensional bounded potential with resonance is given by

$$V(q) = (q^2 - a^2)^2(q^2 - b^2), \tag{6}$$

where a and b are real. For a suitable choice of the parameters (a, b), with $b > a$, the potential exhibits two symmetric external wells separated by a third deeper one (Fig. 2a). In the following, we will systematically work with a non relativistic particle whose mass is taken to unity. The quantum spectrum is purely discrete, bounded from below and the eigenstate $|\psi\rangle$ of energy E is given by the spectral equation

$$\hat{H}|\psi\rangle = E|\psi\rangle \tag{7}$$

where the Hamiltonian is $\hat{H} = H(\hat{p}, \hat{q})$ where $\hat{p}, \hat{q}$ are the momentum and position operators and H the classical Hamiltonian

$$H(p, q) = \frac{p^2}{2} + V(q)\ . \tag{8}$$

2.2 The spectrum

When dealing with a polynomial Hamiltonian, a convenient way to perform the numerical computations is to write directly the canonical operators in the harmonic oscillator eigenbasis (Korsch & Glück, 2002)

$$\hat{q} = \sqrt{\frac{\hbar}{2}} \begin{pmatrix} 0 & \sqrt{1} & 0 & 0 & \cdots \\ \sqrt{1} & 0 & \sqrt{2} & 0 & \cdots \\ 0 & \sqrt{2} & 0 & \sqrt{3} & \cdots \\ 0 & 0 & \sqrt{3} & 0 & \cdots \\ \vdots & \vdots & \vdots & \vdots & \ddots \end{pmatrix}, \hat{p} = \mathrm{i}\sqrt{\frac{\hbar}{2}} \begin{pmatrix} 0 & -\sqrt{1} & 0 & 0 & \cdots \\ \sqrt{1} & 0 & -\sqrt{2} & 0 & \cdots \\ 0 & \sqrt{2} & 0 & -\sqrt{3} & \cdots \\ 0 & 0 & \sqrt{3} & 0 & \cdots \\ \vdots & \vdots & \vdots & \vdots & \ddots \end{pmatrix}. \tag{9}$$

The Hamiltonian (8) is now written in terms of power of these infinite matrices. In practice, one needs to truncate them. First, one computes numerically the products of the truncated matrices and then one sums each terms. One can now diagonalize the Hamiltonian to get the eigenvalues. Numerically, we must finally check that the truncation of these infinite matrices does not affect the results up to the required precision.

The eigenenergies are plotted as a function of the Planck's constant $\hbar$ in figure 2b). Even though it is a standard procedure when one studies quantum phenomena in the semiclassical limit, it is worth to remind that treating the Planck constant as a varying parameter has to be understood as a substitute for varying the physical parameters of the system (for instance, through a rescaling of the quantities including $\hbar$ in order to work with dimensionless parameters). Since $V(-q) = V(q)$, the eigenstates can be classified according to their parity $(\pm)$. Moreover, for small enough $\hbar$, the part of the spectrum

below the local maximum $V_{\max}$ can be divided in two families: first, a family of doublets (E_n^+, E_n^-) that remain positive and below $V_{\max}$ for any value of $\hbar$ (like the red lines in fig. 2b)) and second, a family of energies that eventually become negative for small enough $\hbar$ (like the blue line in fig. 2b)). Except near the special values of $\hbar$ where the two families almost intersect (these crossings will be discussed in the next section) the first family corresponds to states localised in the lateral wells with $E_n^+ \simeq E_n^- \sim \hbar\omega_l(n+1/2)$, with integer n and $\omega_l = \sqrt{V''(a)}$ the harmonic frequency in the bottom of the lateral wells : like in the double-well case, the difference $\Delta E_n \stackrel{\text{def}}{=} |E_n^+ - E_n^-|$ will be our tunnelling splittings between symmetric and antisymmetric states. The energies that make up the second family do not form doublets but rather correspond to states localised in the central well. In the semiclassical limit these energies behave as $E_m^{(c)} = V(0) + \hbar\omega_c(m+1/2) + \mathrm{O}(\hbar^2)$ with integer m and $\omega_c = \sqrt{V''(0)}$ the harmonic frequency in the bottom of the central well.

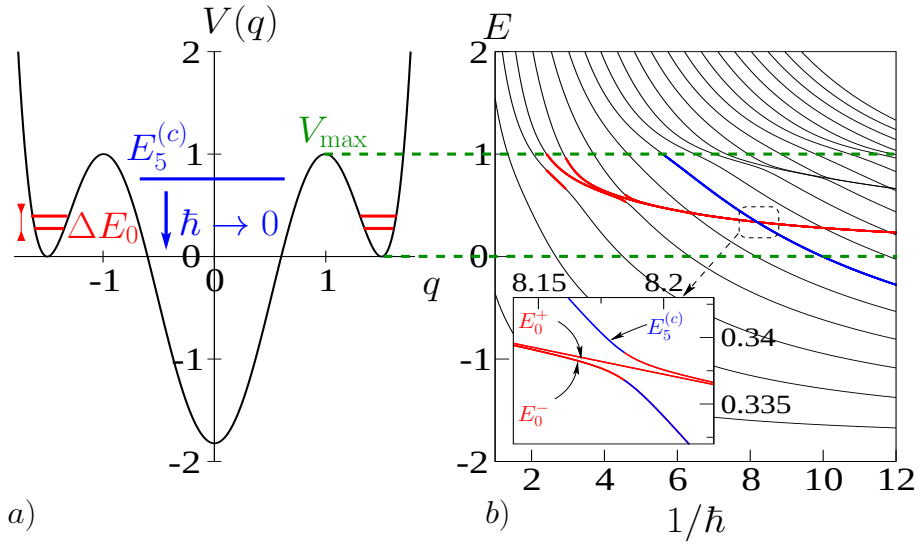

Figure 2: a) The three-well potential (6) for $a = 1.5$ and $b = 0.6$. b) The first 20 energy levels versus $1/\hbar$ (black lines in figure b). The dashed green lines delimit the energy range where the doublets ΔE_n lie. We have also sketched the doublet ΔE_0 (in red) and the level $E_5^{(c)}$ (in blue) associated to the central well. The inset in b) shows the avoided crossing between the three levels E_0^+, E_0^- and $E_5^{(c)}$ that occurs near $1/\hbar \simeq 8.18$.

2.3 Avoided crossings in the spectra

In the absence of singularities (Cohen & Kuharetz, 1993), the spectrum has no degeneracies. When varying a control parameter ($\hbar$ in our case), what appears to be a crossing between energies is actually an avoided crossing if one look at a sufficiently high resolution (see the insert in figure 2b)). More precisely, two energy levels having the same parity seem to repel one from the other and a substitution between one component of the doublet (E_0^-) and $E_5^{(c)}$ occurs

when $1/\hbar$ increases from 8.14 to 8.24. This scenario can be reproduced using a three -level model (§ 3.3) and can be followed using a phase-space representation of the corresponding wave functions (§ 2.4).

Let us note that near such avoided crossings, the definition of the doublet becomes ambiguous: whatever criterion we retain to discriminate between the levels $E_n^{\pm}$ and $E_m^{(c)}$ (for instance the two nearest energies or those states selected from their overlap with a coherent state localised in one of the three wells) a discontinuous switch will occur and the level repulsion originates a large increase, by several of magnitude, of the tunnelling splittings ΔE_n. Those are the resonances seen from the energy levels point of view. The word "resonance" is then to be taken in the usual sense: the strong variation of ΔE within a small range of variation of one parameter $(1/\hbar)$ is directly related to the coincidence between frequencies, namely the frequencies of the Rabi oscillations between the wells. From then on, we will define ΔE_n in selecting the energies involved as the largest overlap between the eigenstates and a coherent state localised in one of the external well. The splitting will thus be computed numerically following this criterion, leading to the figures 3a) and 6. As seen in figure 3a), the simple exponential behaviour (2) breaks down when the doublet is mixed with a third level and some resonant spikes appear. Moreover, these peaks are not differentiable at the values of $\hbar$ corresponding to the discontinuous switches. As ΔE increases close to a resonance, the tunnelling period $T = \hbar/\Delta E$ becomes smaller: a quantum state initially prepared in one of the external wells will then oscillate more rapidly from this well to its symmetric. For some particular values of the parameters, that is to say when an isolated level comes to perturb the doublet, a middle well separating two symmetric wells can thus enhanced significantly the tunnelling[2]. In section 3 we will derivate almost analytical formulas for the splitting and the height of the peaks.

2.4 Husimi representation

It is very illuminating to see the resonance at work using a phase-space representation of the eigenfunctions involved in the triplet $E_n^{\pm}, E_m^{(c)}$ near an avoided crossing. Instead of computing eigenstates in either the $q-$ or $p-$representation, we will choose the Husimi distribution $\psi(p,q)$ which mixes both space and momentum variables and gives the density probability to find a quantum state in the phase space. The Husimi distribution is defined as the square modulus of the projection of the state $|\psi\rangle$ onto a coherent state $|\alpha\rangle$ (Cohen-Tannoudji, Diu & Laloë, 1997, complement G_V). One can use the basis $|n\rangle$ of the harmonic oscillator in order to write the coherent state as follows

$$|\alpha\rangle = \mathrm{e}^{-|\alpha|^2/2} \sum_{n=0}^{\infty} \frac{\alpha^2}{\sqrt{n!}} |n\rangle, \tag{10}$$

where $\alpha \stackrel{\text{def}}{=} (p + \mathrm{i}q)/\sqrt{2\hbar}$, then

$$\psi(p,q) \stackrel{\text{def}}{=} |\langle\alpha|\psi\rangle|^2 = \mathrm{e}^{-|\alpha|^2} \left| \sum_{n=0}^{\infty} \frac{\alpha^2}{\sqrt{n!}} \langle\psi|n\rangle \right|^2 . \tag{11}$$

[2]In more complicated systems which are beyond the scope of this paper, one can observe crossings in the spectra and then the splitting would exhibit antipeaks with infinite height in a semilogarithmic scale. The tunnelling would thus be completely destroyed.

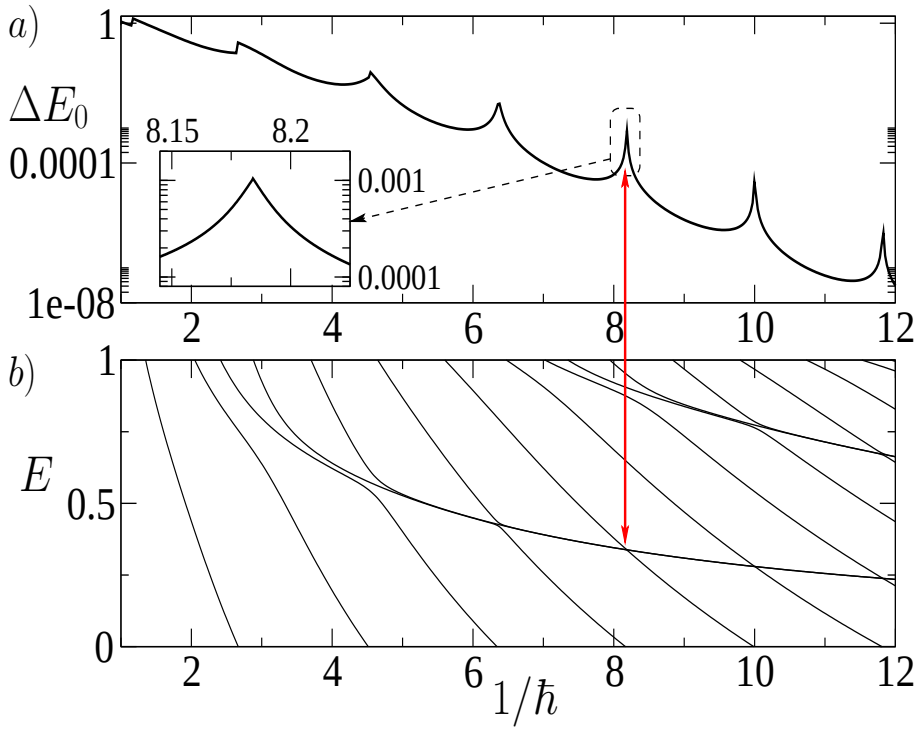

Figure 3: The splitting ΔE_0 is plotted in a) in a semilogarithmic scale versus $1/\hbar$ for the three-well potential (6) with $a = 1.5$ and $b = 0.6$. The figure b) exhibits the associated spectra versus $1/\hbar$. The double arrowed red line indicates the correspondance between avoided crossing in the spectra and resonances in the splitting. The resonance at $\hbar \simeq 1/8.18$ has been magnified in the insert in figure a).

The Husimi distribution $\psi(p, q)$ is definite positive. The coherent state $|\alpha\rangle$ is a Gaussian wavepacket built such that it saturates the uncertainty inequalities i.e. $\Delta p \Delta q = \hbar/2$. A coherent state, also called a quasi-classical state, can be understood as the *most classical* quantum state since it can be shown that the expectation values of the quantum observables follow the same evolution as the corresponding classical ones at the leading order of $\hbar$. Physically, the square of the scalar product of the eigenstate $|\psi\rangle$ and a coherent state can be interpreted as the density probability to find the quantum state in a cell of area $\hbar$ centered at the momentum p and the position q in a coarse-grained phase space. The Husimi distribution appears thus to be an appropriate picture to study quantum dynamics in the semiclassical regime (Novaes, 2003). Far from a resonance (see figure 4a.0), the symmetric and antisymmetric eigenstates related to the doublet with the energies (E_0^+, E_0^-) are mainly localised in the external wells while the isolated level is clearly well-delimited in the middle well as shown in figures 4a.1,2,3). When $1/\hbar$ increases from 8.15 to 8.25, we can follow the exchange between the state corresponding to $E_5^{(c)}$ and the state corresponding to E_0^- while the even state remains almost unaltered and mainly localised in the lateral wells. At the resonance (fig. 4b.1,2,3), the two states with the same parity become

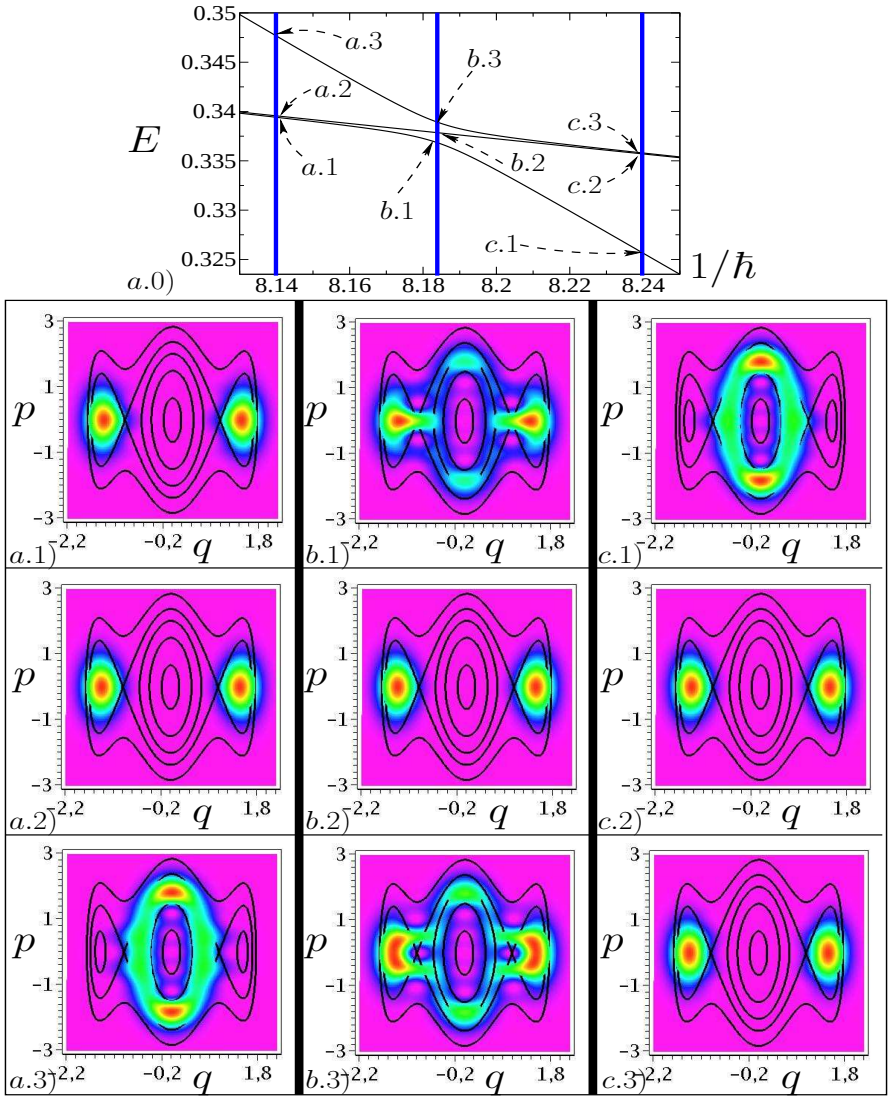

Figure 4: For the three-well polynomial potential (6) with $a = 1.5$ and $b = 0.6$, we have plotted the Husimi distribution for the three levels involved in the avoided crossing around $\hbar \simeq 1/8.18$ (see also insert in figure 2a). The vertical blue lines in respectively a,b,c.0) defines the values of the Planck's constant (resp. $1/\hbar \simeq 8.14, 8.184, 8.24$) and shows the relative position of the energies in the spectra (black lines) where the dashed arrows point out the energy levels related to each Husimi distribution depicted in a,b,c.1,2,3). The classical phase space is also superimposed on the Husimi plots.

intertwined: this is the signature in the phase space of the so-called resonances. For these particular values of the parameters, the odd quantum states leak out through the barriers all over the three wells. We cannot clearly distinguish which odd state is now a part of the doublet and we find the ambiguity concerning the

definition of the splitting again.

3 Almost analytical computations

3.1 Square potential

To go beyond a simple diagonalization and understand analytically the origin of the resonant spikes in the splittings, potential (6) is still difficult to handle. The standard instanton procedure of Wick rotating the time $t \mapsto \mathrm{i}t$ in order to work with a upside-down potential (Coleman, 1985, chap. 7) fails because there remain a barrier to cross when reversing V into $-V$ in figure 2 a). Two of us have recently shown how to generalise the instanton method in the most general $1d$-case (Le Deunff & Mouchet, 2010) and how to recover analytically the effect of resonances but this method goes far beyond the present elementary complement to a first years lecture on quantum physics. To deal with a simpler analytically tractable model let us introduce a three-well piecewise constant potential that will mimic the situation described in the previous section. Therefore we will take (Fig. 5)

$$V(q) = \begin{cases} +\infty & \text{Region 1:} \quad q < -c, \\ 0 & \text{Region 2:} \quad -c < q < -b, \\ V_{\max} & \text{Region 3:} \quad -b < q < -a, \\ V_{\min} & \text{Region 4:} \quad -a < q < a, \\ V_{\max} & \text{Region 5:} \quad a < q < b, \\ 0 & \text{Region 6:} \quad b < q < c, \\ +\infty & \text{Region 7:} \quad c < q. \end{cases} \tag{12}$$

While keeping the essential features of resonances described above, we will then be able to derive analytical formulas in the semiclassical limit for the splitting and the height of the resonance peaks.

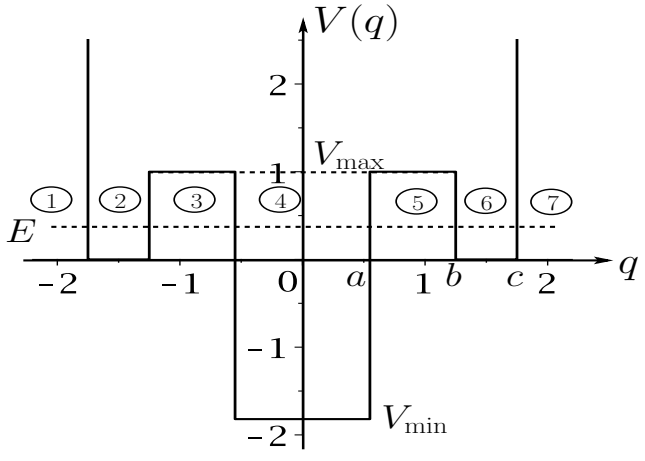

Figure 5: The piecewise three-well square potential defined in (12) with the parameters $a = 0.55$, $b = 1.25$, $c = 1.75$, $V_{\max} = 1.0$ and $V_{\min} = -1.82$.

3.2 Semiclassical transfer matrix approach

In the case of one-dimensional systems, a convenient way to obtain the eigenfunctions and eigenenergies is to use transfer matrix formalism (Walker & Gathwright, 1994) (Azbel, 1983, Appendix A). The transfer matrices connect the amplitudes of the wavefunctions in the different regions of the potential. As we want to compute tunnelling splittings, we will pay particular attention to energies such that $0 < E < V_{\max}$. We will use this approach to get the equations which give the energy levels and secondly to compute the splitting in the semiclassical regime.

3.2.1 Energy quantization

With potential (12), the general solution $\psi(q)$ of the time-independent Schrödinger's equation at energy E, $-\hbar^2\psi''(q)/2 + V(q)\psi(q) = E\psi(q)$, (the prime stands for the derivative) has the form:

$$\begin{cases} \text{Region 1:} & \psi_1(q) = 0, \\ \text{Region 2:} & \psi_2(q) = A_2 \mathrm{e}^{\mathrm{i}k_0 q} + B_2 \mathrm{e}^{-\mathrm{i}k_0 q}, \\ \text{Region 3:} & \psi_3(q) = A_3 \mathrm{e}^{k_{\max} q} + B_3 \mathrm{e}^{-k_{\max} q}, \\ \text{Region 4:} & \psi_4(q) = A_4 \mathrm{e}^{\mathrm{i}k_{\min} q} + B_4 \mathrm{e}^{-\mathrm{i}k_{\min} q}, \\ \text{Region 5:} & \psi_5(q) = A_5 \mathrm{e}^{k_{\max} q} + B_5 \mathrm{e}^{-k_{\max} q}, \\ \text{Region 6:} & \psi_6(q) = A_6 \mathrm{e}^{\mathrm{i}k_0 q} + B_6 \mathrm{e}^{-\mathrm{i}k_0 q}, \\ \text{Region 7:} & \psi_7(q) = 0, \end{cases} \tag{13}$$

where

$$k_0 = \frac{\sqrt{2E}}{\hbar}, \quad k_{\min} = \frac{\sqrt{2(E - V_{\min})}}{\hbar}, \quad k_{\max} = \frac{\sqrt{2(V_{\max} - E)}}{\hbar}. \tag{14}$$

The amplitudes (A_i, B_i) are *a priori* complex numbers. As the energy $E > 0$, the wavefunctions $\psi_2(q)$, $\psi_4(q)$ and $\psi_6(q)$ are linear combinations of two plane waves travelling in opposite directions, while in the regions where the energy is lower than the barrier, $\psi_3(q)$ and $\psi_5(q)$ are combinations of real exponentials. Though the potential $V(q)$ is not continuous, one still requires the eigenfunctions and its derivative to be smooth everywhere and especially at each frontier between two regions, i.e. $q = \{\pm a, \pm b, \pm c\}$. It leads to the following equalities

$$\begin{cases} \psi_2(-c) = 0, & \\ \psi_2(-b) = \psi_3(-b), & \psi_2'(-b) = \psi_3'(-b), \\ \psi_3(-a) = \psi_4(-a), & \psi_3'(-a) = \psi_4'(-a), \\ \psi_4(a) = \psi_5(a), & \psi_4'(a) = \psi_5'(a), \\ \psi_5(b) = \psi_6(b), & \psi_5'(b) = \psi_6'(b), \\ \psi_6(c) = 0. & \end{cases} \tag{15}$$

Using these continuity equations, one can express the amplitudes (A_i, B_i) in terms of any others (A_j, B_j) through the relation

$$\begin{pmatrix} A_i \\ B_i \end{pmatrix} = \mathbf{T}(i,j) \begin{pmatrix} A_j \\ B_j \end{pmatrix}, \qquad \mathbf{T}(i,j) = \begin{pmatrix} \mathbf{T}_{11}(i,j) & \mathbf{T}_{12}(i,j) \\ \mathbf{T}_{21}(i,j) & \mathbf{T}_{22}(i,j) \end{pmatrix}, \tag{16}$$

where $\mathbf{T}(i,j)$ is the transfer matrix from the region j to i. Each transfer matrix can be written using three elementary matrices

$$\begin{cases} \mathbf{u}_\alpha(k) = \begin{pmatrix} \mathrm{e}^{\mathrm{i}k\alpha} & 0 \\ 0 & \mathrm{e}^{-\mathrm{i}k\alpha} \end{pmatrix}, \quad \mathbf{v}_\alpha(k) = \begin{pmatrix} \mathrm{e}^{-k\alpha} & 0 \\ 0 & \mathrm{e}^{k\alpha} \end{pmatrix}, \\ \mathbf{w}(k,\tilde{k}) = \dfrac{1}{2}\begin{pmatrix} 1-\mathrm{i}k/\tilde{k} & 1+\mathrm{i}k/\tilde{k} \\ 1+\mathrm{i}k/\tilde{k} & 1-\mathrm{i}k/\tilde{k} \end{pmatrix}, \end{cases} \tag{17}$$

where k, $\tilde{k}$ and α are real. The matrices $\mathbf{u}$ (resp. $\mathbf{v}$) correspond to the propagation in a classicaly allowed region ($E > V$) (resp. forbidden region, $E < V$); the matrices $\mathbf{w}$ correspond to the continuity equations at one step. We have

$$\mathbf{u}_{-\alpha}(k) = \big[\mathbf{u}_\alpha(k)\big]^{-1}, \qquad \mathbf{u}_\alpha(k)\mathbf{u}_\beta(k) = \mathbf{u}_{\alpha+\beta}(k). \tag{18}$$

and $\mathbf{w}$ fulfills the condition $[\mathbf{w}(k,\tilde{k})]^{-1} = \mathbf{w}^*(\tilde{k},k)$, for real k and $\tilde{k}$, where $\mathbf{w}^*$ denotes the complex conjugate of $\mathbf{w}$. The transfer matrices are given by

$$\begin{aligned} \mathbf{T}(2,3) &= \mathbf{u}_b(k_0)\mathbf{w}(k_{\max},k_0)\mathbf{v}_b(k_{\max}), && (19)\\ \mathbf{T}(3,4) &= \mathbf{v}_{-a}(k_{\max})\mathbf{w}^*(k_{\min},k_{\max})\mathbf{u}_{-a}(k_{\min}), && (20)\\ \mathbf{T}(4,5) &= \mathbf{u}_{-a}(k_{\min})\mathbf{w}(k_{\max},k_{\min})\mathbf{v}_{-a}(k_{\max}), && (21)\\ \mathbf{T}(5,6) &= \mathbf{v}_b(k_{\max})\mathbf{w}^*(k_0,k_{\max})\mathbf{u}_b(k_0). && (22) \end{aligned}$$

Then, the relation between (A_2,B_2) and (A_4,B_4) are given by the transfer matrix :

$$\begin{aligned} \mathbf{T}(2,4) &= \mathbf{T}(2,3)\mathbf{T}(3,4) \\ &= \mathbf{u}_b(k_0)\mathbf{w}(k_{\max},k_0)\mathbf{v}_b(k_{\max})\Big[\mathbf{u}_a(k_{\min})\mathbf{w}(k_{\max},k_{\min})\mathbf{v}_a(k_{\max})\Big]^{-1} \end{aligned} \tag{23}$$

A straightforward computation shows that the elements of the matrix transfer through a barrier have to be such that $\mathbf{T}_{22} = (\mathbf{T}_{11})^*$ and $\mathbf{T}_{21} = (\mathbf{T}_{12})^*$. Since the potential is symmetric, the matrix $\mathbf{T}(2,4)$ contains already all the information about the system. Indeed, noting that

$$\begin{aligned} \mathbf{T}(6,4) &= [\mathbf{T}(4,6)]^{-1} = [\mathbf{T}(5,6)]^{-1}[\mathbf{T}(4,5)]^{-1} \\ &= \mathbf{u}_{-b}(k_0)\mathbf{w}(k_{\max},k_0)\mathbf{v}_{-b}(k_{\max})\Big[\mathbf{u}_{-a}(k_{\min})\mathbf{w}(k_{\max},k_{\min})\mathbf{v}_{-a}(k_{\max})\Big]^{-1}, \end{aligned} \tag{24}$$

and performing the symmetry-axis transformation $(a,b,c) \to (-a,-b,-c)$, the expression (24) is nothing but $\mathbf{T}(2,4)$. We distinguish the parity of the eigenstates with the condition $\psi_4'(0) = 0$ for the even states while the odd ones fulfill $\psi_4(0) = 0$. Using the continuity condition at $q = -c$, it leads to the algebraic system

$$\begin{pmatrix} A_2 \\ -A_2\mathrm{e}^{-2\mathrm{i}k_0c} \end{pmatrix} = \begin{pmatrix} \mathbf{T}_{11}(2,4) & \mathbf{T}_{12}(2,4) \\ (\mathbf{T}_{12}(2,4))^* & (\mathbf{T}_{11}(2,4))^* \end{pmatrix}\begin{pmatrix} A_4 \\ \pm A_4 \end{pmatrix}, \tag{25}$$

where $\pm$ stands for the parity of the eigenstate. The transcendantal equations for the energy levels are thus obtained easily by manipulating the system and eliminating the amplitudes from the previous equalities:

$$\begin{aligned} &\mathrm{Re}\left[(\mathbf{T}_{11}(2,4)+\mathbf{T}_{12}(2,4))\mathrm{e}^{-\mathrm{i}k_0c}\right] = 0 \qquad : \text{even states}, && (26)\\ &\mathrm{Im}\left[(\mathbf{T}_{11}(2,4)-\mathbf{T}_{12}(2,4))\mathrm{e}^{-\mathrm{i}k_0c}\right] = 0 \qquad : \text{odd states}. && (27) \end{aligned}$$

These conditions can be written in a more tractable form for the even states

$$D_+(E) \stackrel{\text{def}}{=} F_+(E) + G_+(E)\mathrm{e}^{-2k_{\max}(b-a)} = 0, \tag{28}$$

and the odd states

$$D_-(E) \stackrel{\text{def}}{=} F_-(E) - G_-(E)\mathrm{e}^{-2k_{\max}(b-a)} = 0, \tag{29}$$

with

$$F_+(E) \stackrel{\text{def}}{=} \Big(k_0\cos[k_0(c-b)] + k_{\max}\sin[k_0(c-b)]\Big) \times\Big(k_{\max}\cos(k_{\min}a) - k_{\min}\sin(k_{\min}a)\Big), \tag{30}$$

$$G_+(E) \stackrel{\text{def}}{=} \Big(k_0\cos[k_0(c-b)] - k_{\max}\sin[k_0(c-b)]\Big) \times\Big(k_{\max}\cos(k_{\min}a) + k_{\min}\sin(k_{\min}a)\Big), \tag{31}$$

$$F_-(E) \stackrel{\text{def}}{=} \Big(k_0\cos[k_0(c-b)] + k_{\max}\sin[k_0(c-b)]\Big) \times\Big(k_{\min}\cos(k_{\min}a) + k_{\max}\sin(k_{\min}a)\Big), \tag{32}$$

$$G_-(E) \stackrel{\text{def}}{=} \Big(k_0\cos[k_0(c-b)] - k_{\max}\sin[k_0(c-b)]\Big) \times\Big(k_{\min}\cos(k_{\min}a) - k_{\max}\sin(k_{\min}a)\Big). \tag{33}$$

The zeroes of $D_\pm(E)$ give the exact discrete energies $E = E_n^\pm$ for the three-well square potential.

In the semiclassical limit, the height of the barrier is much larger than the energies and the term of order one in the sums (28) and (29) dominate the decreasing exponential, so the energies can be approximated keeping only the first term

$$D_+(E) \underset{\hbar\to 0}{\sim} F_+(E) = 0, \tag{34}$$

$$D_-(E) \underset{\hbar\to 0}{\sim} F_-(E) = 0. \tag{35}$$

Within this approximation, tunnelling is neglected. There are two possible ways to cancel (34) or (35) as the functions $F_+(E)$ and $F_-(E)$ are written as a product of two functions

$$F_+(E) = F_{\mathfrak{e}}(E) \times F_{\mathfrak{m},+}(E), \tag{36}$$

$$F_-(E) = F_{\mathfrak{e}}(E) \times F_{\mathfrak{m},-}(E), \tag{37}$$

with

$$\begin{cases} F_{\mathfrak{e}}(E) \stackrel{\text{def}}{=} k_0\cos[k_0(c-b)] + k_{\max}\sin[k_0(c-b)], \\ F_{\mathfrak{m},+}(E) \stackrel{\text{def}}{=} k_{\max}\cos(k_{\min}a) - k_{\min}\sin(k_{\min}a), \\ F_{\mathfrak{m},-}(E) \stackrel{\text{def}}{=} k_{\min}\cos(k_{\min}a) + k_{\max}\sin(k_{\min}a). \end{cases} \tag{38}$$

The factor $F_{\mathfrak{e}}(E)$ appears in both cases (even and odd) and corresponds to the quantization condition in the lateral wells in the limit $b-a \to +\infty$ and provide the average position e_n of the doublets. The second factors $F_{\mathfrak{m},\pm}(E)$ in (36) and (37) are nothing but the transcendantal equations which lead respectively to the even and odd energy levels $e^{\pm}_{\mathfrak{m}}$ of the finite square well (Merzbacher, 1970, chap. 6, § 8) and approximate the energies related to the central well of (12). It is clear that, in the limit where we do not care about tunnelling, the energies associated to the external wells are degenerate as both quantization conditions (34) and (35) share the same first factor. Avoided crossings also disappear as the two factors of $F_+(E)$ (resp. $F_-(E)$) in (36) (resp. (37)) vanish simultaneously for some particular values[3] of $\hbar$.

3.2.2 Semiclassical formulas for the splitting

To recover the exponentially fine structure of the spectra that caracterise tunnelling, let us expand the right hand side of the exact quantization conditions (28) and (29) around the average value of the doublet that has been determined above $E_n^{\pm} = e_n + \epsilon_n^{\pm}$

$$\begin{aligned} D_+(e_n+\epsilon_n^+) &\simeq D_+(e_n) + \epsilon_n^+ D'_+(e_n) + \mathrm{o}((\epsilon_n^+)^2) = 0, \qquad (39)\\ D_-(e_n+\epsilon_n^-) &\simeq D_-(e_n) + \epsilon_n^- D'_-(e_n) + \mathrm{o}((\epsilon_n^-)^2) = 0, \qquad (40) \end{aligned}$$

Keeping only the exponentially dominant terms, we get

$$\Delta E_n = |E_n^- - E_n^+| = |\epsilon_n^- - \epsilon_n^+| \underset{\hbar\to 0}{\sim} \left| \frac{G_-(e_n)}{F'_-(e_n)} + \frac{G_+(e_n)}{F'_+(e_n)} \right| \mathrm{e}^{-2k_{\max}(b-a)} \qquad (41)$$

where $F'_{\pm}(e_n) = F'_{\mathfrak{e}}(e_n) \times F_{\mathfrak{m},\pm}(e_n)$. One recovers on average the exponentially small behaviour of the splitting. Noting that $p = \hbar k$ where k is equal to the expressions in (14), the argument of the exponential is nothing but the classical action under the two barriers of the potential

$$\int_{-b}^{-a} p\mathrm{d}q + \int_a^b p\mathrm{d}q = 2\int_a^b p\mathrm{d}q = 2\hbar k_{\max}(b-a). \qquad (42)$$

While $F'_{\mathfrak{e}}(e_n) \neq 0$, one denominator in (41) may still vanish when $F_{\mathfrak{m},\pm}(e_n) = 0$ which provides a condition for determining the resonances. To fix the divergences in (41) and get a finite value of the height of the spikes, we have to go to the next order in the Taylor expansions (39) and (40). We distinguish both cases depending on whether the third level is even or odd. If the resonance is due to an even level $e^+_{\mathfrak{m}}$ then $F'_+(e_n) = 0$ and we need to expand $D_+(e_n+\epsilon_n^+)$ to the second order. The splitting is of order $\mathrm{o}[\mathrm{e}^{-2k_{\max}(b-a)}]$ but it is no longer true close to a resonance where it becomes much larger because of the prefactor which is no longer of order one. The dominant terms are thus now of order $\mathrm{o}[(\epsilon_n^+)^2]$ and $\mathrm{o}[\mathrm{e}^{-2k_{\max}(b-a)}]$ while it is still sufficient to keep only the first order term for the odd condition $D_-(e_n+\epsilon_n^-)$, as previously. In case an odd energy level is responsible for a divergence in (41), we proceed similarly with the odd

[3] For these particular values of $\hbar$, some zeros of the conditions (34) and (35) are of order 2 and give the average positions of the actual avoided crossings, otherwise they are all of order one.

condition $D_-(e_n+\epsilon_n^-)$. Collecting all the results we get

$$\begin{aligned}\Delta E_{n,+} &\underset{\hbar\to 0}{\sim} \left|\frac{G_-(e_n)}{F'_-(e_n)}\mathrm{e}^{-2k_{\max}(b-a)} - \sqrt{\frac{-2G_+(e_n)}{F''_+(e_n)}}\mathrm{e}^{-k_{\max}(b-a)}\right|,\\ &\underset{\hbar\to 0}{\sim} \left|\sqrt{\frac{-2G_+(e_n)}{F''_+(e_n)}}\right|\mathrm{e}^{-k_{\max}(b-a)},\end{aligned} \tag{43}$$

and

$$\begin{aligned}\Delta E_{n,-} &\underset{\hbar\to 0}{\sim} \left|\sqrt{\frac{2G_-(e_n)}{F''_-(e_n)}}\mathrm{e}^{-k_{\max}(b-a)} + \frac{G_+(e_n)}{F'_+(e_n)}\mathrm{e}^{-2k_{\max}(b-a)}\right|,\\ &\underset{\hbar\to 0}{\sim} \left|\sqrt{\frac{2G_-(e_n)}{F''_-(e_n)}}\right|\mathrm{e}^{-k_{\max}(b-a)},\end{aligned} \tag{44}$$

where $\Delta E_{n,+}$ (resp. $\Delta E_{n,-}$) is the height of a resonance caused by an even (resp. odd) level from the central well. The denominators $F''_\pm(e_n)$ can be again simplified and written as the product $2F'_{\mathfrak{c}}(e_n)\times F'_{\mathfrak{m},\pm}(e_n)$ when the level $e^\pm_{\mathfrak{m}}$ is equal to e_n (at the resonance). The argument of the exponential in the splitting formula (41) far from resonances is twice the argument in (43) and (44). The semiclassical formula (41) shows a very good agreement with the exact results as plotted in figure 6. The semiclassical predictions are more and more accurate for large values of $1/\hbar$ even around the resonances where the height of the peaks is very well predicted by the formulas (43) and (44).

3.3 Matrix model

We want to obtain a matrix model of tunnelling in a potential with several wells, as the one of equation (6). A solution is to represent the Hamiltonian in a basis of "quasi-modes" coupled by tunnelling. Clearly, tunnelling is a wave phenomenon which couples two adjacent wells classically separated by a finite barrier. If there was no tunnelling at all, then each well would have its own independant eigenmodes, approximately given by JWKB ansatz based on the real quantizing classical tori. In the semiclassical limit, tunnelling is a vanishing effect, and these JWKB modes become very good local approximations of the exact solutions of the time independant Schrödinger equation, that is, the exact eigenmodes. For this reason, these JWKB ansatz are often called "quasi-mode" in this context. But, if one sticks to real classical tori, then tunnelling is not taken into account by these approximations. On the other hand, one can consider tunnelling as a small coupling between quasi-modes.

For each well of the potential, we hence define a quasi-modes family ϕ_n, with quasi-energies E_n. In the simple case of a symmetric double-well, one has quasi-modes ϕ^l_n with energies E^l_n, associated with the left well; and quasi-modes ϕ^r_n with energies E^r_n, associated with the right well. Because of classical symmetry, both are degenerate, that is, $E^l_n = E^r_n$, but tunnelling lifts this degeneracy in the exact spectrum. Close to energy E^l_n, the Hamiltonian is well described by a two level system in the basis of the two corresponding quasi-modes. For instance, close to the ground state, one has

$$H \simeq \begin{pmatrix} E_0 & \delta \\ \delta & E_0 \end{pmatrix}, \tag{45}$$

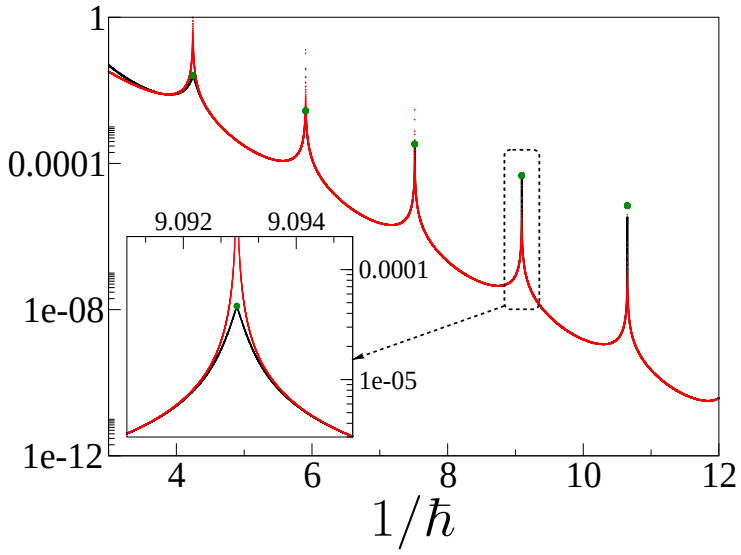

Figure 6: The splitting for the ground state is plotted in a semilogarithmic scale versus $1/\hbar$ for the piecewise constant potential defined in (12) with the parameters $a = 0.55$, $b = 1.25$, $c = 1.75$, $V_{\max} = 1.0$ and $V_{\min} = -1.82$. The black line is the exact computation obtained by solving numerically the exact quantization conditions (28) and (29). The red line corresponds to the semiclassical formula (41) and the green dots show the height of the resonances computed with (43) and (44). The insert is a magnification of the resonance at $\hbar \simeq 1/9.093$.

where δ gives the coupling strength induced by tunnelling between the two quasi-modes. Diagonalisation of this matrix gives two eigenstates, an odd one and an even one,

$$\psi_\pm = \frac{1}{\sqrt{2}} \left(\phi_0^l \pm \phi_0^r \right), \tag{46}$$

associated with two eigenenergies

$$E_\pm = E_0 \pm \delta. \tag{47}$$

In this model, the tunnel splitting is therefore given by

$$\Delta E = 2\delta. \tag{48}$$

Consistency with JWKB analysis and equation (2) is obtained by chosing $2\delta = \alpha\hbar e^{-A/\hbar}$.

It is easy to generalise this simple model to a triple well like (6) by defining three families of quasi-modes : ϕ_n^l, ϕ_n^c and ϕ_n^r. Now we focus on the situation shown on figure 4. In the language of this model, it is an avoided crossing involving a doublet $\left(\phi_n^l, \phi_n^r\right)$ with degenerate quasi-energy E_n^l, and a state ϕ_m^c with quasi-energy E_m^c which is close to E_n^l. As $\hbar$ is tuned, E_m^c crosses E_n^l, but tunnel coupling makes it an avoided-crossing. In the region of this avoided crossing, one can restrict the Hilbert space, in the same spirit as in (Tomsovic & Ullmo, 1994), to a subspace spanned by these three states, that we now name

without label in order to simplify notation : ϕ_l and ϕ_r with energy E, and ϕ_c with energy E'. In this basis one has something like

$$H \simeq \begin{pmatrix} E & \delta & 0 \\ \delta & E' & \delta \\ 0 & \delta & E \end{pmatrix}. \tag{49}$$

Notice that there is no direct coupling from the left well to the right one, and only remains tunnelling from left to centre and from centre to right. In order to match with § 2.4, realistic values of these coefficients would be

$$E = \hbar\omega_l(n+\frac{1}{2}) \tag{50}$$

$$E' = V(0) + \hbar\omega_c(m+\frac{1}{2}) \tag{51}$$

$$\delta = \alpha\hbar e^{-A/\hbar}. \tag{52}$$

It is easy to compute the corresponding eigenenergies :

$$E_1 = \frac{E+E'}{2} - \frac{1}{2}\sqrt{(E-E')^2+8\delta^2} \tag{53}$$

$$E_2 = E \tag{54}$$

$$E_3 = \frac{E+E'}{2} + \frac{1}{2}\sqrt{(E-E')^2+8\delta^2}. \tag{55}$$

In figure 7, we have plotted these values as a function of $1/\hbar$ by using expressions (50), (51) and (52).

When $E'-E \gg \delta$, one has

$$E_1 \simeq E - \frac{\delta^2}{2|E-E'|} \tag{56}$$

$$E_2 = E \tag{57}$$

$$E_3 \simeq E' + \frac{\delta^2}{2|E-E'|}. \tag{58}$$

This corresponds to the situation of figure 4a.0) where only direct tunnelling is involved, and the central state has little influence. The splitting of the doublet $E_2 - E_1$ is of the order δ^2, that is, $e^{-2A/\hbar}$, which is basically the product of two transfer coefficients through one barrier.

When $E-E' \gg \delta$, one has

$$E_1 \simeq E' - \frac{\delta^2}{2|E-E'|} \tag{59}$$

$$E_2 = E \tag{60}$$

$$E_3 \simeq E + \frac{\delta^2}{2|E-E'|}. \tag{61}$$

This time, the energy of the central state ϕ_c has crossed the doublet, which now corresponds to $E_3 - E_2$, as in the situation of figure 4a.3).

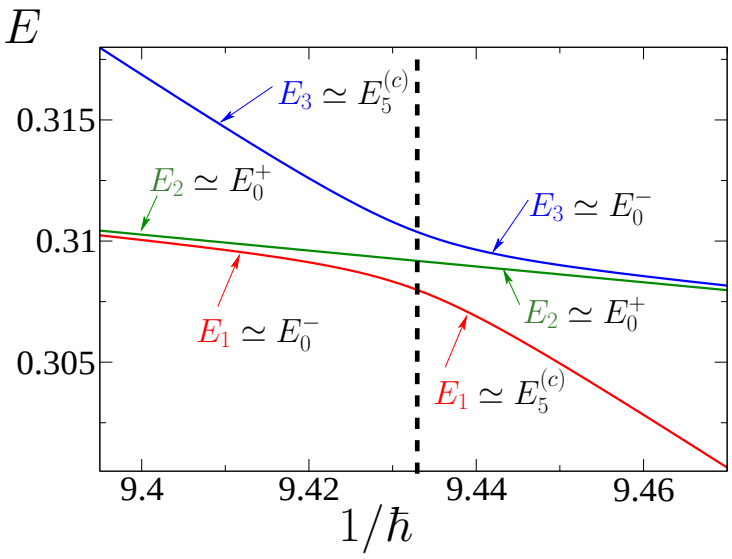

Figure 7: Avoided crossing modelised with a 3 levels system. We have used $\omega_l = 5.833, \omega_c = 3.656, n = 0, m = 5, V(0) = -1.8225, \alpha = 0.197$ and $A = 0.34$. The vertical black dashed line indicates the value of $\hbar$ at the resonance condition $E = E'$. The numerical values are chosen according to the parameters used in figures 2 and 4.

The situation of figure 4a.2) corresponds to the value of $\hbar$ for which the central state has resonance $E = E'$ with the lateral ones, and one then has

$$E_1 = E - \sqrt{2}\delta \quad (62)$$

$$E_2 = E \quad (63)$$

$$E_3 = E + \sqrt{2}\delta. \quad (64)$$

The splitting then reaches its maximum $\Delta E = 2\sqrt{2}\delta$, of the order $e^{-A/\hbar}$ which is consistent with (43) and (44). Resonance with the central state thus facilitates tunnelling, by one order of magnitude, between the two non-adjacent wells.

4 Conclusion

While tunnelling in one dimensional time-independent systems can hardly offers some surprises, it remains sufficiently rich to provide a warming up for dealing with much more elaborate situations that occurs in higher dimensions (or when adding an explicit time dependency). In the latter cases, tunnelling frequencies or rates generically fluctuate by several order of magnitudes; understanding these fluctuations, that can be seen as an intricate overlap of resonances — still qualitatively very different from what occurs in one-dimension—, is the aim of a vivid field of actual researches both theoretically and experimentally (Keshavamurthy & Schlagheck, 2011) and many issues still remain unclear. The two three-well models we have studied in this paper present the simplest bounded situation where tunnelling deviates from the usual purely exponential behaviour and is indeed drastically enhanced near resonances.

References

Azbel, M. Y. (1983). Eigenstates and properties of random systems in one dimension at zero temperature, Phys. Rev. B **28**(8): 4106–4125.

Bender, C. M. & Orszag, S. A. (1978). Advances Mathematical Methods for Scientists and Engineers, Springer-Verlag, New York. Reprinted by Springer-Verlag (1999).

Bohm, D. (1951). Quantum theory, Prentice Hall, Englewood Cliffs, N. J.

Born, M. & Wolf, E. (1980). Principles of Optics, Pergamon Press, Oxford. (6th edition).

Brillouin, L. (1926). La mécanique ondulatoire de Schrödinger; une méthode générale de résolution par approximations successives, C. R. Acad. Sci. Paris **183**: 24–26. (in french).

Cohen, J. M. & Kuharetz, B. (1993). Energy level degeneracy, Journal of Mathematical Physics **34**: 12–22.

Cohen-Tannoudji, C., Diu B. & Laloë, F. (1997). Mécanique quantique, Tome 1, Hermann, Paris. (in french).

Coleman, S. (1985). Aspects of symmetry, Cambridge University Press.

Eigler, D. M. & Schweizer, E. K. (1990). Positioning single atoms with a scanning tunnelling microscope, Nature **344**: 524–526.

Fowler, R. & Nordheim, L. (1928). Electron emission in intense electric fields, Proc. Roy. Soc. London Ser. A **119**: 173–181.

Gamow, G. (1928). Zur quantentheorie des atomkernes, Zts. f. Phys. **51**((3-4)): 204–212. (in german).

Garg, A. (2000). Tunnel splittings for one-dimensional potential wells revisited, Amer. J. Phys. **68**(5): 430.

Granot, E. (2006). Resonant tunnelling and the transition between quantum and classical domains, Eur. J. Phys. **27**: 985–993.

Gurney, R. W. & Condon, E. U. (1928). Wave mechanics and radioactive disintegration, Nature **122**: 439.

Hund, F. (1927a). Zur deutung der molekelspektren. i, Zts. f. Phys. **40**(10): 742–764. (in german).

Hund, F. (1927b). Zur deutung der molekelspektren. iii., Zts. f. Phys. **43**(11-12): 805–826. (in german).

Jeffreys, H. (1925). On certain approximate solutions of linear differential equations of the second order, Proc. London Math. Soc. (2nd ser.) **23**: 428–436.

Keshavamurthy, S. & Schlagheck, P. (eds) (2011). Dynamical tunneling. Theory and experiment, CRC Press, Taylor and Francis,, Boca Raton.

Korsch, H. J. & Glück (2002). Computing quantum eigenvalues made easy, Eur. J. Phys. **23**: 413–426.

Kramers, H. A. (1926). Wellenmechanik und halbzahlige quantisierung, Zts. f. Phys. **39**: 828–840. (in german).

Landau, L. D. & Lifshitz, E. M. (1958). Quantum Mechanics (non relativistic theory), Vol. 3 of Course of Theoretical Physics, Pergamon Press, Oxford.

Le Deunff, J. & Mouchet, A. (2010). Instantons re-examined: Dynamical tunneling and resonant tunneling, Phys. Rev. E **81**: 046205.

Merzbacher, E. (1970). Quantum Mechanics, John Wiley, New York. 2nd edition.

Merzbacher, E. (2002). The early history of quantum tunneling, Phys. Today **55**(8): 44–50.

Messiah, A. (1959). Mécanique Quantique (2 vol.), Dunod, Paris. English translation by G. M. Stemmer: North-Holland (Amsterdam).

Nordheim, L. (1927). Zur theorie der thermischen emission und der reflexion von elektronen an metallen, Zts. f. Phys. **46**(11-12): 833. (in german).

Novaes, M. (2003). Wigner and Husimi functions in the double-well potential, J. Opt. B: Quantum Semiclass. Opt. **5**: 342.

Schlagheck, P., Mouchet, A. & Ullmo, D. (2011). Resonance-assisted tunneling in mixed regular-chaotic systems, in Keshavamurthy & Schlagheck (2011). Chap. 8.

Tomsovic, S. & Ullmo, D. (1994). Chaos-assisted tunneling, Phys. Rev. E **50**: 145–162.

Walker, J. S. & Gathwright, J. (1994). Exploring one-dimensional quantum mechanics with transfer matrices, Amer. J. Phys. **62**(5): 408–422.

Wentzel, G. (1926). Eine Verallgemeinerung der Quantenbedingungen für die Zwecke der Wellenmechanik, Zts. f. Phys. **38**: 518–529. (in german).